



# A novel frequency protection interval adjustment method based on Doppler frequency offset pre-compensation for space-based Internet of Things\*

Qingquan LIU<sup>†1</sup>, Lihu CHEN<sup>††1</sup>, Songting LI<sup>1</sup>, Yiran XIANG<sup>1</sup>, Baokang ZHAO<sup>2</sup>

<sup>1</sup>College of Aerospace Science and Engineering, National University of Defense Technology, Changsha 410073, China

<sup>2</sup>College of Computer, National University of Defense Technology, Changsha 410073, China

<sup>†</sup>E-mail: liuqq\_wy2022@163.com; chenlihu05@nudt.edu.cn

Received Jan. 14, 2024; Revision accepted May 16, 2024; Crosschecked

**Abstract:** The space-based Internet of Things (IoT) requires more frequency resources so that it becomes possible for a large number of users to access the network. However, the frequency resources that are currently available have already been allocated to a great extent. Furthermore, the utilization rate of the allocated frequency resources is low. In order to realize a greater number of users accessing the network under restricted conditions of frequency resources, this work proposes a scheme based on Doppler frequency offset (DFO) pre-compensation to improve the utilization rate of spectrum resources. By calculating the relative motion between the satellite and the transmitting terminal, combined with the length and transmission rate of the message, the optimal compensation value of the Doppler frequency deviation is determined. Realize the reduction of the frequency-protection interval. The simulation results show that the pre-compensation method can expand the user access volume by 90%–400 times. The proper selection of the pre-compensation used for calculating the number of compensations and the transmission rate can also help increase the incremental user access by an additional 45% or more. This method improves the spectrum utilization and provides a solution to the challenge of access by a large number of users.

**Key words:** Protection interval; Spectrum utilization; Doppler frequency offset pre-compensation; Massive access users

<https://doi.org/10.1631/FITEE.2400033>

**CLC number:** TN927

## 1 Introduction

Space-based Internet of Things (IoT) is an effective compensation and extension of the ground-based IoT. It utilizes various types of space-based platforms to realize the acquisition, processing, transmission, and application of IoT information. It has become a fundamental technical means for building the interconnection of all things and for ubiquitous sensing. The space-based IoT system has the ad-

vantages of being able to realize global coverage, all-weather operation, and strong stability. It has been widely used in logistics monitoring, transportation, environmental protection, hydrological monitoring, and in other fields (Chen et al., 2022; Yang et al., 2022; Li et al., 2023; Yu et al., 2024a). However, the frequency resources that need to be relied upon for space-based IoT work are currently facing two prominent problems. One is the scarcity of the remaining frequency resources that can be used for division, and the Ku frequency band, as the “golden frequency band” for low-orbit satellite communication, has almost been completely allocated. The second aspect is that the divided frequency resources have not been used aptly or the utilization rate is low, and most of

<sup>‡</sup> Corresponding author

\* Project supported by the Proximity Space Science, Technology and Industry Guidance Fund(No. LKJJ-2023022-01)

ORCID: Qingquan LIU, <https://orcid.org/0009-0002-1761-5602>; Lihu CHEN, <https://orcid.org/0000-0002-9160-1981>

© Zhejiang University Press 2024

the divided frequency resources are in an idle state (Tang et al., 2018). Literature (Yang, 2019) lists that the average spectrum utilization rate of different frequency bands <3 GHz provided by the shared spectrum to the National Science Foundation is only 5.2% (Fcc, 2002). About 31.25% of the total number of sub-band carriers in the IEEE802.15.3c standard are blank carriers (Ge et al., 2016). Meanwhile, the Global System for Mobile Communications Association predicted that the global scale of IoT connections in 2025 will reach 24.6 billion (Centenaro et al., 2021), and more than 100 million users will have access to the satellite terminals. Therefore, the development of space-based IoT is also facing the new technical challenge of how to meet the needs of massive user access under the conditions of restricted spectrum resources.

Literature Chen et al. (2022) and Liu et al. (2021), respectively, proposed that in the context of spectrum-resource constraints, increasing the user access requires the study of efficient and high-throughput multiple access techniques and the improvement of the utilization of limited spectrum resources. Currently, the commonly used multiple access techniques are Frequency Division Multiple Access (FDMA) (Deng et al., 2018), Space Division Multiple Access (SDMA) (Yao et al., 2018), Time Division Multiple Access (TDMA) (Vahideh and Hassan, 2009), Code Division Multiple Access (CDMA) (Wang et al., 2022), and so on. Methods to improve the spectrum utilization are through the use of cognitive radio technology (Zhang et al., 2017), cellular multiplexing (Jabbari et al., 2010), and tapping into the use of higher frequency bands, such as the development of millimeter wave technology (Lei et al., 2023). StarLink, the second-generation system of SpaceX in the United States, achieves improved spectrum utilization by sharing the spectrum with other space-based and terrestrial users. Furthermore, its new-generation satellite system communication bands are all Ku and Ka bands (Liu et al., 2020). In addition, SpaceX is also acquiring more spectrum resources through acquisitions and other means.

FDMA is a commonly used multiple access technique. Specifically, the FDMA technique works by dividing the channel frequency band into a number of narrower mutually exclusive sub-bands. Each sub-band is divided for the exclusive use of one user.

When dividing the sub-frequency bands, it is necessary to leave a certain frequency-protection interval. This is done to avoid the neighboring channel interference due to the Doppler frequency offset (DFO) generated by the relative motion of the satellite and the ground terminal.

It is mentioned in the literature (Li, 2023) that the DFO of a low-orbit satellite with an orbital altitude of 500 km will generate a frequency deviation of 12.6~14.2 kHz. Since the bandwidth and power resources of satellites are limited, leaving a certain frequency-protection interval to avoid neighboring channel interference will result in low bandwidth utilization to a certain extent. This results in less data being able to be output, as well as fewer users being allowed into the network.

Diao et al. (2012) and Liu et al. (2015, 2023) propose to utilize the two-line orbital element (TLE) of the satellite message, combined with the relevant orbital uptake model, to carry out orbital computation for any satellite with a known TLE message. Mao (2020) proposes a code-aided high DFO calculation method with low BER. Wang et al. (2017) proposes an estimation algorithm for the joint carrier frequency offset and carrier phase offset. Zhang et al. (2021) and Liu and Zhu (2017) propose methods to eliminate the Doppler frequency from the leading sequence and adjusting the frame structure, respectively. However, the improvement in the number of users accessing the network is limited.

The effects of delay and DFO in star~ground links have been studied by Mao (2020), but the solutions given cannot flexibly adjust the subcarrier spacing according to the actual situation. DFO compensation has also been studied by Zhang et al. (2021) and Liu and Zhu (2017), but the improvement in user access is limited. Dynamic fitting of DFO functions to predict and compensate for highly dynamic terminals has been proposed by Hou et al. (2015). However, realizing the real-time fitting of the function requires the real-time computation of the Greenwich Mean Time, which requires higher computational performance and energy consumption of the terminal. Yao et al. (2021) and Yu et al. (2023, 2024b)) propose the use of edge computing and computing power network to assist in dealing with large-scale resource-scheduling problems to alleviate the central node computational pressure.

Inspired by the above literature, this paper pro-

poses a spectrum resource-utilization scheme based on the DFO pre-compensation by using the idea of edge computing. It aims to address the problem of the high requirements for satellite performance in the way of DFO compensation on the star when the satellite faces massive terminal access. Pre-compensation of the wide range of frequency deviations generated by the Doppler shift is carried out by means of a ground terminal. It achieves the purpose of reducing the frequency-protection interval, improving the spectrum-utilization efficiency and the access volume of space-based IoT users, and realizing that there is no need to pass the fitting function. This reduces the energy requirements and delays the service life of terminals, especially those located in areas that are off the beaten track, such as those in harsh geographical environments.

The rest of the paper is organized as follows: Section 2 presents the proposed system model. Section 3 discusses the proposed DFO pre-compensation method. The simulation and performance analysis of the proposed method is presented in Section 4. Finally, we summarize the approximate flow and the advantages and disadvantages of the method.

## 2 System model

### 2.1 Vector model of the relative position and the relative velocity of a low-orbit satellite and a ground terminal

Using the SGP4 model, through the TLE of the satellite and the position of the ground terminal in longitude  $L$ , latitude  $B$  and elevation  $H$ , as well as the motion state and direction of motion, the position and velocity vectors of the satellite and the ground terminal in the earth centered inertial (ECI) coordinate system can be obtained as  $\vec{R}_{sat}$ ,  $\vec{V}_{sat}$ ,  $\vec{R}_g$  and  $\vec{V}_g$ , respectively.

The relative position  $\vec{r}$  and the relative velocity  $\vec{v}$  of the satellite and the ground terminal are:

$$\vec{r} = \vec{R}_{sat} - \vec{R}_g = \begin{bmatrix} r_x \\ r_y \\ r_z \end{bmatrix}, \vec{v} = \vec{V}_{sat} - \vec{V}_g = \begin{bmatrix} v_x \\ v_y \\ v_z \end{bmatrix} \quad (1)$$

### 2.2 DFO model

Ground terminals and LEO satellites will generate DFO due to relative motion during satellite

communication. The relative motion between the LEO satellite and the various types of terminals is shown in Fig.1.

According to the definition of Doppler shift, the DFO  $f_{Doppler}$  generated by the relative motion between the ground terminal and the satellite is shown in Eq.(2) below:

$$f_{Doppler} = f_{up} \cdot \frac{v}{c} \cdot \cos \beta \quad (2)$$

$$\cos \beta = \frac{\vec{r} \cdot \vec{v}}{|\vec{r}| \cdot |\vec{v}|}, \beta \in (0, \pi) \quad (3)$$

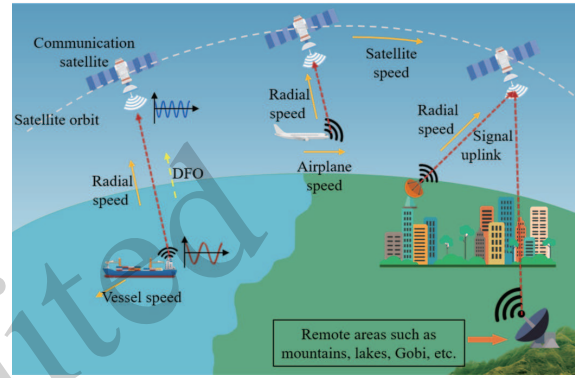


Fig. 1 Schematic diagram of the relative motion of the LEO satellite and various types of terminals

where,  $f_{up}$  is the frequency of the signal sent from the ground terminal to the LEO satellite,  $v$  is the relative velocity between the ground terminal and the LEO satellite,  $c$  is the speed of light, and  $\beta$  is the angle between the signal transmission direction and the radial motion.

The frequency of the signal received at the receiving end on the star is shown in Eq.(4).

$$f = f_{up} \pm f_{Doppler} \quad (4)$$

### 2.3 Channel segmentation model

Under a certain total bandwidth  $B_0$ , channel segmentation needs to take into account the channel bandwidth and isolation band required by the user. Among them, the channel bandwidth  $B_1$  is related to the transmitted symbol rate  $R_s$ , the code rate  $R_c$ , and the de-roll factor  $\alpha$ .

$$B_1 = \frac{R_s(1 + \alpha)}{R_c} \quad (5)$$

In order to avoid the DFO from interfering with neighboring channels, a protection interval  $B_p$  is required. Therefore, the required bandwidth  $B$  for a

single user is:

$$B = B_1 + B_p = B_1 + 2f_{Doppler} \quad (6)$$

The final number of channels that can be divided is:

$$Num = \lfloor B_0/B \rfloor \quad (7)$$

### 3 Spectrum resource-utilization technique based on DFO pre-compensation

The technical scheme proposed in this paper to improve the utilization efficiency of spectrum resources is shown in Fig.2. Firstly, the ground terminal calculates the relative motion parameters of the satellite and the ground terminal at the moment of message transmission through the TLE and SGP4 orbit model of the satellite. Then, according to the message length and transmission rate selected by the ground terminal, the number of message splits is judged and the value of the DFO pre-compensations is computed. The transmitted signal is then compensated with the optimal DFO compensation value. Next, the frequency-protection interval, which was originally set so large to prevent frequency interference due to DFO, is adjusted and reduced. Finally, the channel resources are reallocated to accommodate more users and improve the spectrum utilization.

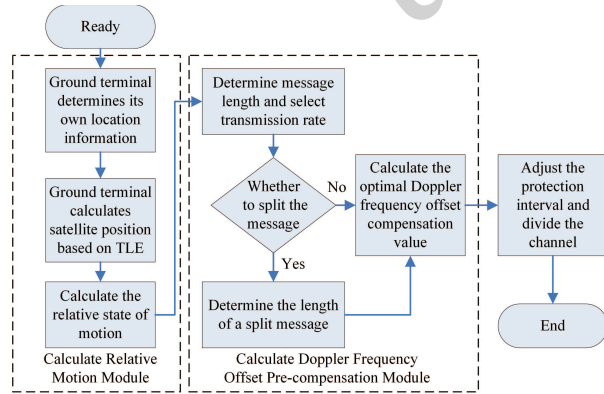


Fig. 2 Spectrum resource-utilization scheme based on DFO pre-compensation. DFO, Doppler frequency offset

#### 3.1 Determination of the Doppler frequency deviation protection interval

It is a continuous process for the ground terminal to send message signals to the receiving end of

the LEO satellite. The duration is shown in Eq.(8). During the message-sending process, the relative position relationship between the LEO satellite and the ground terminal is constantly changing. The DFO generated by the relative motion is also changing. Combined with Eqs (2) and(3) it's change rule can be expressed by Eq.(9).

$$T = \frac{N}{R_s} \quad (8)$$

$$\frac{df_{Doppler}}{dt} = \frac{f_{up}}{c} \cdot \frac{d(v \cos \beta)}{dt} = \frac{f_{up}}{c} \cdot \frac{dv_r}{dt} \quad (9)$$

where  $T$  is the message-sending duration,  $N$  is the message length, and  $v_r$  is the radial component of the relative velocity. Also, the relative motion between the satellite and the ground terminal is:

$$r = \sqrt{R_{sat}^2 + R_g^2 - 2R_{sat}R_g \cos \alpha} \quad (10)$$

$$v_r = \frac{dr}{dt} = \frac{R_{sat}R'_g - R_gR'_{sat} - (R_gR'_{sat} + R_{sat}R'_g) \cos \alpha}{\sqrt{R_{sat}^2 + R_g^2 - 2R_{sat}R_g \cos \alpha}} - \frac{R_{sat}R_g \frac{d \cos \alpha}{dt}}{\sqrt{R_{sat}^2 + R_g^2 - 2R_{sat}R_g \cos \alpha}} \quad (11)$$

$\alpha$  is the angle between the ground terminal and the satellite about the center of the earth, due to the fact that the orbital altitude of the LEO satellite is  $<2000$  km, and  $\alpha_{max} = \arccos\left(\frac{R_E}{R_{sat}}\right) = 0.7058 \text{ rad}$ . Also, in the message transmission time  $T$  is much smaller than the orbital period, so the effect of the earth's rotation can be ignored, and the distance between the satellite and the ground terminal from the center of the earth can be approximated as constant. Thus, Eq. (11) can be simplified as:

$$v_r = -\frac{R_{sat}R_g}{r} \frac{d \cos \alpha}{dt} = \frac{R_{sat}R_g \sin \alpha}{r} \frac{d\alpha}{dt} \quad (12)$$

$$\frac{dv_r}{dt} = \frac{R_{sat}R_g}{r} \left( \cos \alpha \left( \frac{d\alpha}{dt} \right)^2 + \sin \alpha \frac{d^2\alpha}{dt^2} \right) - \frac{R_{sat}R_g^2}{r^3} \left( \sin^2 \alpha \left( \frac{d\alpha}{dt} \right)^2 \right) \quad (13)$$

Since the orbit design of LEO communication satellites is mostly an approximate circular orbit, and according to the relationship between the three sides of an obtuse triangle, it is easy to obtain  $r^2 \cos \alpha \geq R_{sat}R_g \sin^2 \alpha$ ,  $\alpha \leq \alpha_{max}$ . Thus the change in  $f_{Doppler}$  is related to  $\alpha$ . The process of  $\alpha$  decreasing to 0 and then increasing corresponds to the process of the satellite moving closer to and then farther away from the terminal, and  $f_{Doppler}$  while increasing with  $r$ .

Therefore, the frequency-protection interval needs to consider the DFO changes during the whole message-transmission time. As shown in Fig. 3, it is the ideal case that the DFO is fully compensated. The signal frequency received by the receiver on the star has no DFO. There is no need to set additional protection intervals, and the frequency resources can be fully utilized for channel segmentation.

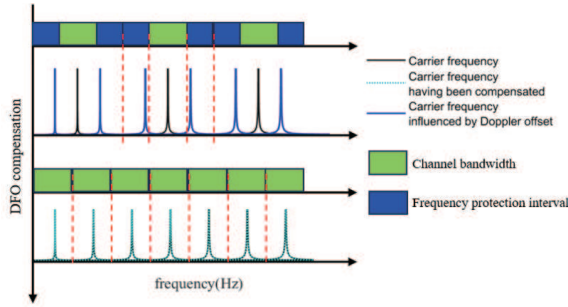


Fig. 3 Protection interval setting after DFO compensation in the ideal case. DFO, Doppler frequency offset.

In practice, the full realization of DFO pre-compensation requires real-time calculation and adjustment of the compensation value for the whole transmitting process. The realization of this process requires high power consumption of the signal transmitting terminal, high arithmetic power requirements, and harsh conditions for the ground terminal equipment. However, without the DFO pre-compensation, the large protection interval greatly reduces the utilization efficiency of frequency resources. Comprehensively considering the performance conditions of the terminal equipment, the method of calculating the DFO once and compensating continuously is adopted.

The ground terminal calculates the time period covered by the LEO satellite beam. Then the DFO  $f_{Doppler,1}, f_{Doppler,2}$  generated by the uplink of the signal frequency at the beginning moment  $t_1$  and the ending moment  $t_2$  of the ground terminal being covered and the applied DFO compensation value  $f_c$  are calculated respectively. Then the protection interval  $\Delta f$  of the DFO is set as shown in Eq. (14).

$$\Delta f = \max(|f_c - f_{Doppler,1}|, |f_c - f_{Doppler,2}|) \quad (14)$$

### 3.2 Determination of the optimal compensation frequency for Doppler frequency deviation

The size of the DFO protection interval is changed when the moment of choosing to calculate the DFO is different. Through research and analysis, the DFO of the LEO satellite has the same change rule in the two motion processes of approaching and moving away from the ground terminal. So the process of the LEO satellite moving away from the ground terminal is selected to determine the optimal pre-compensation frequency of DFO.

The DFO pre-compensation value can be calculated by selecting the start  $t_1$ , middle  $t_0$ , and end moments of the message  $t_2$ ,  $t_1 < t_0 < t_2, r_1 < r_0 < r_2$ . From Eqs (9) and (12), the DFO is increasing during message transmission.

$$f_{Doppler,1} \leq f_{Doppler} \leq f_{Doppler,2} \quad (15)$$

Without DFO pre-compensation, the required bandwidth to avoid mutual interference between the channels is  $[f_{up} - f_{Doppler,2}, f_{up} + f_{Doppler,2}]$ . The DFO protection interval is set to  $\Delta f = \max(f_{Doppler}) = f_{Doppler,2}$ . The DFO compensation value  $f_c$  that can be applied is:

$$0 \leq f_c \leq f_{Doppler,2} \quad (16)$$

Overcompensation can also lead to channel interference when  $f_{Doppler} < f_c$ . An additional protection interval  $\Delta f' = f_c - f_{Doppler}$  is also required. Therefore, the DFO protection interval  $\Delta f$  needs to be satisfied when  $t_1 \leq t \leq t_2$ .

$$f_{up} + f_c + \Delta f = f_{up} + f_{Doppler}(t) \quad (17)$$

Substituting Eqs (15) and (16) into Eq. (17) yields:

$$\frac{f_{Doppler,2} - f_{Doppler,1}}{2} \leq \Delta f \leq f_{Doppler,2} \quad (18)$$

In order to get as many new channels as possible,  $\sum_{t_1 \leq t \leq t_2} |f_{Doppler}(t) - f_c|$  needs to be minimized.

The protection interval  $\Delta f_{\min} = \frac{f_{Doppler,2} - f_{Doppler,1}}{2}$  needs to be set when  $f_c = \frac{f_{Doppler,2} + f_{Doppler,1}}{2}$ . This is the optimal compensation frequency for DFO:

$$f_{c,best} = \frac{f_{Doppler,2} + f_{Doppler,1}}{2} \quad (19)$$

### 3.3 Determination of the number of message splits

As shown in Eqs (9) and (13), the DFO generated by the relative motion between the LEO satellite and the ground terminal is mainly affected by the satellite's orbital characteristics, and it changes continuously with time. Therefore, the effect of the message-transmission time, which is mainly determined by the message length and transmission rate, needs to be considered in the DFO pre-compensation.

When the transmission rate is certain and the message length sent by the terrestrial terminal is short, the purpose of improving spectrum utilization can be achieved without splitting the message. However, when the message length sent by the terminal is long, it is still necessary to set a large DFO protection interval without splitting the message and performing DFO calculation only once.

Therefore, we set the transmission time threshold  $\tau = \frac{T}{n}$ , and the accuracy thresholds  $\varepsilon$ ,  $n$  for the number of message splits and are satisfied:

$$\tau_n - \tau_{n+1} < \varepsilon \quad (20)$$

As shown in Fig.4, when the ground terminal transmits the message time  $T > \tau$ , the original long message is split into several short messages. The number of split short messages is continuously adjusted to make it meet the requirements of  $T_1, T_2, T_3, \dots, T_n \leq \tau$ .

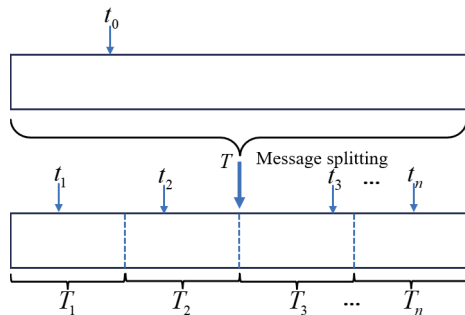


**Fig. 4 Schematic diagram of splitting a long message into multiple short messages**

Selected appropriate DFO values to compensate for the split short messages in turn according to Eqs (16) and (18), and the new protection interval  $\Delta f$

after splitting should satisfy Eq. (21).

$$\Delta f = \max(|f_{Doppler,i1} - f_{c,i}|, |f_{c,i} - f_{Doppler,i2}|) \quad (i = 1, 2, \dots, n) \quad (21)$$

Where  $f_{c,i}$  is the DFO pre-compensation value for the  $i^{th}$  short message.

However, more message splitting is not better. While considering the reduction of the protection interval, it is also important to consider the computational time complexity. Higher time complexity means that the method requires more computation. In order to avoid the resource loss caused by excessive message splitting, the splitting measure is set. The time complexity of the proposed method is:

$$O(n) = n \log_{10}(\log_{10} \varepsilon) \quad (22)$$

It means that the optimal number of message splits changes with the different  $\varepsilon$  settings.

## 4 Experimental simulation and result analysis

### 4.1 Parameter configuration

A ground-fixed sensor, a low-speed moving vessel and a civil aviation airplane in high-speed cruising state are selected as ground terminals. The simulation-related parameters are shown in Table 1.

**Table 1 Distribution of ground terminals**

Terminal type	Longitude (°)	Latitude (°)	Elevation (m)	Velocity (m/s)
Ground-fixed sensors	112.3840	26.7147	68.5453	0
Low-speed vessels	123.8612	30.057	0	15.4333
Civilian plane	123.8900	30.4321	10668	250

A LEO satellite with normal operation in orbit is selected as the satellite receiving end. The maximum angle of the satellite antenna beam is set to 60°. The TLE message parameters of the LEO satellite are shown in Table 2.

According to the simulation needs, three different message lengths of 25 bytes, 50 bytes and 100 bytes, as well as four different symbol rates of 1 kbps, 512 bps, 256 bps and 128 bps are set. The QPSK modulation is used. The roll-off coefficients  $\alpha = 0.5$

**Table 2** STARLINK satellite ephemeris

STARLINK-1007								
1	44713U	19074A	23303.80866486	0.00002495	00000+0	18641-3	0	9999
2	44713	53.0535	91.2629	0001292	85.1075	275.0062	1215.06381831219168	

are set, and the signal transmits at a frequency of 12 GHz with a bandwidth of 10 MHz.

#### 4.2 Comparison of the effect of pre-compensation on the improvement of subscriber access

Firstly, the DFO patterns of three different types of terminals are compared and analyzed, as shown in Fig. 5. It can be seen that the different deployment of terminal positions and different moving speeds only have an impact on the size of the resulting DFO value. However, the change rule of DFO is the same. Therefore, for the convenience of the research, the fixed terminal is selected in the following for the comparison experiment of the effect of DFO pre-compensation on the improvement of the number of access users.

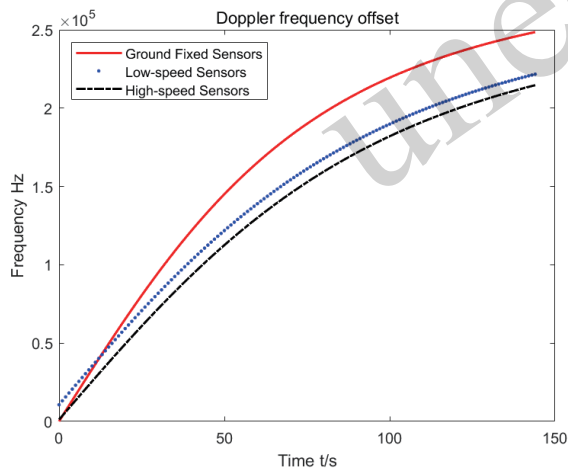


**Fig. 5** DFO over time for different terminal types. DFO, Doppler frequency offset.

##### 4.2.1 The effect of the same message length at different transmission rates

The ground terminal is simulated to send messages of 25 bytes in length at randomly selected times at four symbol element rates of 128 bps, 256 bps, 512 bps and 1 kbps. Compared the number of users accessed in the case of no compensation,

pre-compensation for DFO, and ideal no DFO, and the number of users that can be accessed more by reclassifying the channel with idle frequency after performing compensation. The results are shown in Fig. 6.

The simulation experiments show that while transmitting the 25-byte short message at 128 bps, 256 bps, 512 bps, and 1 kbps codeword rates, the number of access users can be increased by up to 4036, 6525, 7430, and 5481, respectively, by performing DFO calculations once and compensating. By means of DFO pre-compensation, the frequency originally used as a protection interval is released and used to be divided into channels, so that the number of access users after compensation has been substantially increased by about 252, 407, 464, and 342 times compared with that without compensation. Also, the optimal compensation value determined by using Eq. (19) allows the access user quantity increase by 48% compared to the general method.

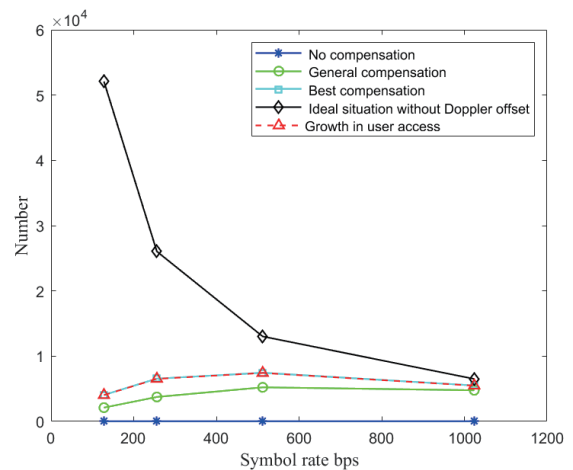


**Fig. 6** Variation in the number of DFO pre-compensated access users at different symbol element rates

Meanwhile, as the symbol element rate increases, the number of users accessed after pre-compensation gradually converges to the number of users accessed under the ideal no-DFO. This is due to the fact that the signal bandwidth is positively

correlated with the transmission rate of the symbol elements. A lower symbol element rate can divide more channels when re-dividing the channels on the frequency bandwidth left free after DFO pre-compensation.

However, for the case of smaller symbol element rate, more time is required to transmit the same length of message. The DFO generated by the relative motion between the LEO satellite and the terminal during transmission is also changing with time. This results in a larger DFO even after pre-compensation. It is still necessary to set a large protection interval to protect the neighboring frequencies from interference with each other. So, it results in a decrease in the incremental number of reduce the increase of access users. Therefore, the higher the symbol element rate, the shorter the transmission time and the less the DFO is affected by the relative motion. The closer the compensated increase in the number of access users is to the ideal situation, the better the result is.

#### 4.2.2 Effect of the same transmission rate at different message lengths

DFO pre-compensation is also performed for the same transmission rate at three different message lengths, 25 bytes, 50 bytes and 100 bytes, and the growth of access users is obtained by comparison, as shown in Fig. 7.

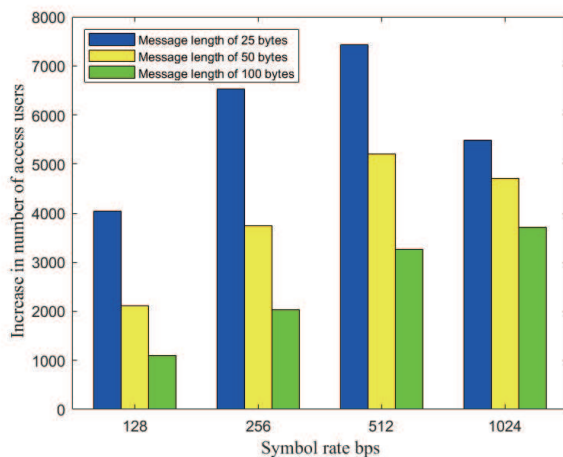


**Fig. 7** DFO pre-compensated access user increment for different message lengths. DFO, Doppler frequency offset.

Comparative analysis reveals that the shorter the message length, the larger the increment in

the number of users after DFO pre-compensation at the same codeword rate. Their average access users increase about 225, 152 and 98 times, respectively. It can be concluded that the method of pre-compensation by calculating the DFO value at one time for terrestrial terminals is better than that for long messages to enhance the effect of short messages.

It is also found that at a certain transmission rate, the effect of DFO pre-compensation on increasing the number of access users increases as the rate increases. However, when the short message is sent at 512 bps and 1024 bps, the number of increased users has a decreasing trend. This is because the bandwidth required for message transmission is related to the symbol element transmission rate as shown in Eq. (5). When transmitting a 25-byte message at a symbol element rate of 512 bps and 1 kbps, the pre-compensated frequency protection intervals are set to 286.54Hz and 139.83Hz, respectively. While the bandwidths required for transmitting a short message are 768 Hz and 1536 Hz, respectively. The signaling bandwidths increase with the symbol rate, resulting in the reduction of the number of channels to be divided. This in turn leads to a decrease in the number of users that can be added by DFO pre-compensation. Therefore, the choice of the symbol element rate is not as large as possible.

#### 4.2.3 Compensation effect for the number of long message splits

In order to further improve the spectrum utilization, it needs to compensate for the shortcomings of the long transmission time leading to the growth of access users differing greatly from the ideal situation. The scheme of splitting the message is proposed for the message whose transmission time is too long. The message with long transmission time is split into several short messages. Also, the DFO is calculated for each short message and pre-compensated separately. This method of message splitting can be used on messages of different lengths and transmission rates.

In this experiment, a 100-byte length message transmitted at 128bps, which is most affected by the transmission time, is selected for research and analysis.  $\varepsilon = 0.005$  is set. The optimal DFO compensation value is obtained according to Eq. (19) and the protection interval is set with Eq. (21). The simulation



results are shown in Fig. 8.

Therefore, six splits of a 100-byte message transmitted at 128 bps to calculate the DFO pre-compensation value provides the best compensation. The number of accessed users increases by about 35.6% compared to the unsplit message with a corresponding length and transmission rate. It can be seen that splitting the message several times does help to increase the number of access users and has less impact on the time complexity.

Finally, the time complexity of the centralized DFO compensation on the satellite, the pre-compensation of the real-time fitted DFO function at the ground terminal, and the DFO pre-compensation scheme proposed in the paper are compared with the growth of message transmission time.

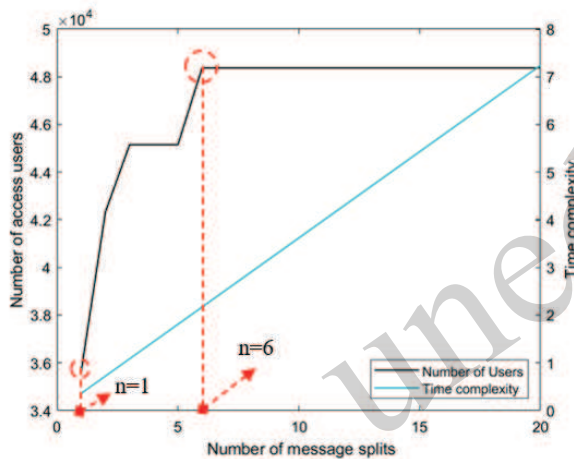


Fig. 8 Relationship between the number of message splits and the number of access users and time complexity.

From Fig. 9, it can be seen that if the idea of edge computing is not adopted, the time complexity of the operation on the satellite will increase with the increase in the number of access users. As for the terrestrial terminal, if the real-time prediction of DFO is used to compensate, its time complexity will increase with the growth of message transmission time. However, the compensation method proposed in this paper does not need to predict the DFO in the whole process. Instead, the number of message splits that should be performed at the corresponding transmission rate and message length can be set for the terminal in advance. Then the DFO at the corresponding moment is predicted, which greatly reduces the computation amount. Also, it can be

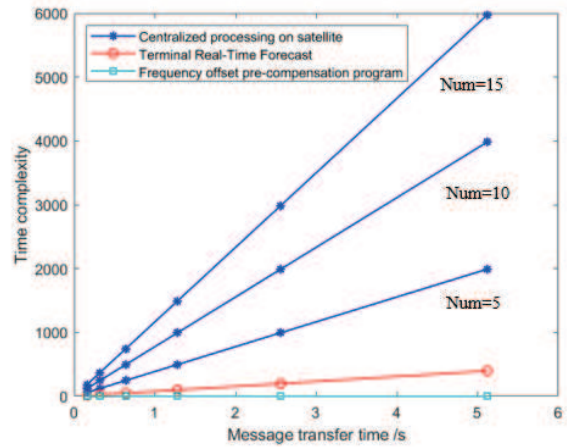


Fig. 9 Variation of time complexity with transmission time for the three methods.

seen from Fig. 6 that the gap between the number of users after its pre-compensation and the number of users in the ideal state gradually decreases with the increase of the symbol element rate. Meanwhile, the time complexity is related to the computational amount. The smaller computational amount of this method makes the energy consumption of the ground terminal reduced and the service life of the terminal located in unfavorable environments is extended.

## 5 Conclusion

In this paper, a spectrum utilization scheme based on the DFO pre-compensation is proposed to address the need to set a large protection interval for preventing frequency interference caused by the DFO, which is generated by the relative motion between LEO satellites and ground terminals. This technical scheme utilizes the idea of edge computing. Firstly, the ground terminal extrapolates the relative motion between the LEO satellite and the ground terminal based on the TLE message. Then, according to the actual needs of the mission, the appropriate length of the message and transmission rate are selected. From there, the number of times a message needs to be split and the optimal DFO pre-compensation value are determined. Finally, the frequency-protection interval is readjusted and new channels are divided. Three message lengths and four symbol rate schemes that can be used in combination with each other are given, which can increase the number of users accessing the network by up to about 400 times. The utilization efficiency of spec-

trum resources is greatly improved. This provides a scheme for the next step to better solve the problem of terrestrial extremely massive user access.

Compared with the real-time fitting of the DFO function, this scheme makes the required computation volume smaller and the computation time requirement lower by sacrificing part of the channel resources. It extends the service life of ground terminals in remote areas and better meets the needs of space-based IoT user terminals in remote and harsh environments. However, this scheme will greatly rely on the TLE data from the satellite, and the TLE data stored in the terminal needs to be updated periodically.

### Contributors

Qingquan Liu and Lihu Chen designed the research. Qingquan Liu processed the data. Qingquan Liu drafted the manuscript. Songting Li, Yiran Xiang and Baokang Zhao helped organize the manuscript. Qingquan Liu, Lihu Chen and Baokang Zhao revised and finalized the paper.

### Compliance with ethics guidelines

Qingquan Liu, Lihu Chen, Songting Li, Yiran Xiang and Baokang Zhao declare that they have no conflict of interest.

### Data availability

The data that support the findings of this study are available from the corresponding author upon reasonable request.

### References

- Centenaro M, Costa CE, Granelli F, et al., 2021. A survey on technologies, standards and open challenges in satellite IoT. *IEEE Commun Surv Tut*, 23(3):1693-1720. <https://doi.org/10.1109/COMST.2021.3078433>
- Chen LH, Cui JW, Li ST, 2022. Key technologies and application prospects for space-based internet of things. *Space Int*, (1):26-32 (in Chinese).
- Deng QY, Li ZT, Chen JB, et al., 2018. Dynamic spectrum sharing for hybrid access in OFDMA-based cognitive femtocell networks. *IEEE Trans Veh Technol*, 67(11):10830-10840. <https://doi.org/10.1109/TVT.2018.2869755>
- Diao NH, Liu JQ, Sun CR, et al., 2012. Satellite orbit calculation based on SGP4 model. *Remote Sens Inform*, 27(4):64-70 (in Chinese). <https://doi.org/10.3969/j.issn.1000-3177.2012.04.011>
- FCC, 2002. Spectrum Policy Task Force. Technical Report, ET Docket No.02-135. Federal Communications Commission, Washington.
- Ge LJ, Li Y, Tao J, 2016. Time and frequency synchronization scheme for IEEE 802.15.3c OFDM system. *J Commun*, 11(2):143-148. <https://doi.org/10.12720/jcm.11.2.14-3-148>
- Hou HL, Chen YJ, Ding S, et al., 2015. Estimation and compensation method for the Doppler frequency shift of high dynamic terminal in LEO satellite communication system. *J Comput Inform Syst*, 11(15):5717-5728. <https://doi.org/10.12733/jcis15259>
- JABBARI B, PICKHOLTZ R, NORTON M, 2010. Dynamic spectrum access and management [Dynamic Spectrum Management]. *IEEE Wirel Commun*, 17(4):6-15. <https://doi.org/10.1109/MWC.2010.5547916>
- Lei HJ, Zhou S, Park KH, et al., 2023. Outage analysis of millimeter wave RSMA systems. *IEEE T Green Commun*, 71(3):1504-1520. <https://doi.org/10.1109/TCOMM.2023.3235349>
- Li K, Li F, Yang WM, 2023. Space-based internet of things: basic concepts, system architecture and development trends. *Telecommun Eng*, 63(2):281-290 (in Chinese). <https://doi.org/10.20079/j.issn.1001-893x.211207003>
- Li ZJ, 2023. Design of low earth orbit space-based internet of things systems. *Mob Commun*, 47(7):98-103 (in Chinese). <https://doi.org/10.3969/j.issn.1006-1010.20230214-0001>
- Liu K, Zhu LD, 2017. Research on the random access technology of LTE based satellite mobile communications. *Radio Commun Technol*, 43(2):12-15 (in Chinese). <https://doi.org/10.3969/j.iss.1003-3114.2017-02.03>
- Liu SJ, Xu FJ, Liu LY, et al., 2020. Introduction of Starlink second generation system. *Satell Network*, 12:62-65 (in Chinese).
- Liu X, Huang C, Cui YQ, et al., 2015. Research on Doppler frequency-shift compensation method based on SGP4 model in satellite communication systems. *Sci Technol Eng*, 15(21):154-158 (in Chinese). <https://doi.org/10.3969/j.issn.1671-1815.2015.21.030>
- Liu YJ, Li BC, Wang YZ, 2021. Key issues in development and application of the sky-based internet of things. *Space Integr Ground Inform Netw*, 2(1):81-86 (in Chinese). <https://doi.org/10.11959/j.issn.2096-8930.2021011>
- Liu YQ, Li HG, Shi JL, et al., 2023. Doppler frequency offset pre-compensation algorithm based on mixed forecast for LEO satellite communications. *Chin High Technol Lett*, 33(6):559-567 (in Chinese). <https://doi.org/10.3772/j.issn.1002-0470.2023.06.001>
- Mao X, 2020. Research on synchronization and access technologies for satellite OFDM systems. MS Thesis, National Key Laboratory of Science and Technology on Communications, Chengdu, China (in Chinese). <https://doi.org/10.27005/d.cnki.gdzku.2020.001565>
- Tan X, Wang H, Fu LZ, et al., 2018. Collision detection and signal recovery for UHF RFID systems. *IEEE T Autom Sci Eng*, 15(1):239-250. <https://doi.org/10.1109/TASE.2016.2614134>
- Vakil V, Aghaeinia H, 2009. Throughput analysis of STS-based CDMA system with variable spreading factor in non-frequency selective Rayleigh fading channel. *Comput Electr Eng*, 35(4):528-535. <https://doi.org/10.1016/j.compeleceng.2008.08.001>

- Wang C, Cui GF, Wang WD, et al., 2017. Joint estimation of carrier frequency and phase offset based on pilot symbols in quasi-constant envelope OFDM satellite systems. *China Commun*, 14(7):184-194. <https://doi.org/10.1109/CC.2017.8019135>
- Wang X, Chen HH, Liu XQ, et al., 2022. Complementary coded CDMA with multi-layer quadrature modulation. *IEEE Trans Veh Technol*, 71(3):2991-3007. <https://doi.org/10.1109/TVT.2022.3142939>
- Yang H, Yuan JQ, Li C, et al., 2022. BrainIoT: Brain-like productive services provisioning with federated learning in industrial IOT. *IEEE Internet Things J*, 9(3):2014-2024. <https://doi.org/10.1109/JIOT.2021.3089334>
- Yang Y, 2019. Research on Decision-Making Mechanism for Improving Adaptability of Cognitive Radio. PhD Dissertation, Harbin Institute of Technology, Shenzhen, China (in Chinese).
- Yao QY, Yang H, Zhu RJ, et al., 2018. Core, mode, and spectrum assignment based on machine learning in space division multiplexing elastic optical networks. *IEEE Access*, 6:15898-15907. <https://doi.org/10.1109/ACCESS.2018.2811724>
- Yao QY, Yang H, Bao BW, et al., 2021. Federated transfer learning-based data security assurance in edge optical networks for IoT applications. Proceedings of Asia Communications and Photonics Conference, p.1-3.
- Yu A, Yang H, Feng CY, et al., 2023. Socially-aware traffic scheduling for edge-assisted metaverse by deep reinforcement learning. *IEEE Network*, 37(6):74-81. <https://doi.org/10.1109/MNET.2023.3317108>
- Yu TK, Yang H, Nie JL, et al., 2024a. Bias-compensation augmentation learning for semantic segmentation in UAV networks. *IEEE Internet Things J*, 11(12):21261-21273. <https://doi.org/10.1109/JIOT.2024.3373454>
- Yu TK, Yang H, Yao QY, et al., 2024b. Multi-visual-GRU-based survivable computing power scheduling in metro optical networks. *IEEE T Netw Serv Man*, 21(1):1302-1315. <https://doi.org/10.1109/TNSM.2023.3314272>
- Zhang JY, Yu ZY, Zhu M, et al., 2021. Design of carrier synchronization algorithm for SCMA system in LEO satellite communication. *Syst Eng Electron*, 43(5):1354-1360 (in Chinese). <https://doi.org/10.12305/j.issn.1001-506X.2021.05.24>
- Zhang L, Xiao M, Wu G, et al., 2017. A survey of advanced techniques for spectrum sharing in 5G networks. *IEEE Wirel Commun*, 24(5):44-51. <https://doi.org/10.1109/MWC.2017.1700069>